Characteristics of the Ion Pressure Tensor in the Earth's Magnetosheath

Xinlin Li[1], H. R. Lewis[1], J. LaBelle[1], T.-D. Phan[2], R. A. Treumann[3]

Abstract. AMPTE/IRM satellite data are used to examine characteristics of the ion pressure tensor in the earth's magnetosheath. The eigenvalues and principal axes of the pressure tensor are computed, and the directions of the principal axes are compared to the direction of the independently measured magnetic field **B**. When the pressure tensor is anisotropic, as is usually the case in the magnetosheath, one of its eigenvalues is observed to be distinguishable from the other two, which are about equal to one another. Thus, the eigenvector associated with the distinguishable eigenvalue defines an axis of symmetry of the pressure tensor. The symmetry axis is generally not parallel to **B**. New features of the plasma distribution function are revealed by using the actual eigenvalues of the pressure tensor rather than the usual $p_\perp$ and $p_\parallel$, where $\perp$ and $\parallel$ denote directions perpendicular and parallel to **B**.

Introduction

In this letter we report preliminary results of an analysis of ion distribution function measurements from the AMPTE/IRM satellite. The original motivation of the study was to examine the nature of empirical closure relations in the earth's magnetosheath that would allow a second or third velocity moment to be expressed in terms of lower moments. As a first step, we have examined the properties of the ion pressure tensor.

Various studies have been made of closure relations in space plasmas, beginning with the work of Feldman et al. [1973] using solar wind measurements. Assuming isotropic pressure and a polytropic law in the plasma sheet, Baumjohann and Paschmann [1989] and Huang et al. [1989] determined values for the polytropic index. Belmont and Mazelle [1992] and Mazelle and Belmont [1993] showed from theoretical arguments and data analysis that a global index generally is not valid and that the double polytropic indices depend on which waves are present and on the nature of the particle distribution functions.

In the magnetosheath region, there has been considerable interest in finding empirical relations among velocity moments. From AMPTE/CCE data under highly compressed conditions (magnetopause $<8.8\ R_E$), Anderson et al. [1994] identified an empirical relation, $T_\perp/T_\parallel = 1 + 0.85\beta_\parallel^{-0.48}$. From AMPTE/IRM crossings of the magnetosheath (apogee of 18.7 R_E), Hill et al. [1994] found the marginal mirror instability criterion for a Maxwellian plasma, $T_\perp/T_\parallel = 1 + \beta_\perp^{-1}$, to be satisfied

[1] Dartmouth College, Hanover, New Hampshire

[2] Herzberg Institute of Astrophysics, Ottawa, Canada

[3] MPI für Extraterrestrische Physik, Garching, Germany

in an average sense. Phan et al. [1994] further demonstrated that the criterion is met throughout the magnetosheath, except in the plasma depletion layer adjacent to the low-shear magnetopause where β is less than unity. Hau et al. [1993], also using AMPTE/IRM data, argued that thermodynamic properties in the magnetosheath can be better described in terms of two polytropic laws: $p_\perp/\rho B^{\gamma_\perp - 1} = C_\perp$ and $p_\parallel B^{\gamma_\parallel - 1}/\rho^{\gamma_\parallel} = C_\parallel$.

In order to study the characterization of a real plasma in terms of fluid variables, such as density, velocity, and pressure, we average the particle distribution function over a time window of width τ. This average is useful for defining fluid variables if $f[\mathbf{r}(t), \mathbf{v}, t]$ is well approximated by the form, $f[\mathbf{r}(t), \mathbf{v}, t] = f^{(0)}[\mathbf{r}(t), \mathbf{v}, t] + f^{(1)}[\mathbf{r}(t), \mathbf{v}, t]$, where $f^{(0)}[\mathbf{r}(t), \mathbf{v}, t]$ varies on a timescale long compared to τ and $f^{(1)}[\mathbf{r}(t), \mathbf{v}, t]$ varies over times short compared to τ. In that case, $\langle f[\mathbf{r}(t), \mathbf{v}, t]\rangle_\tau = f^{(0)}[\mathbf{r}(t), \mathbf{v}, t]$. For a given value of τ, we calculate moments of the averaged distribution function. The statistics presented in this paper of quantities derived from moments of the averaged distribution function are insensitive to the value of τ in the range of 5 to 40 satellite spin periods. (The spin period is about 4.35s; for instrumental reasons, τ is restricted to be a multiple of five times the satellite spin period.)

Two major results of our study are: 1) The ion pressure tensor is nearly always anisotropic. 2) One of its principal axes is approximately a symmetry axis, but that axis is generally not parallel to the magnetic field.

Data Acquisition and Presentation

The three-dimensional ion distribution function was measured on the AMPTE/IRM satellite by a top-hat sensor. The energy range of the instrument is 20 eV/q - 40 keV/q. The ion density, flow velocity, pressure tensor, and heat flux vector were calculated for each spin period under the assumption that only protons were present in the ion population. If another ion species is present, e.g., He^{2+}, its velocities will be overestimated by a factor $\gamma = [(m_a/m_p)/z_a]^{1/2}$ (where m_a and z_a are the ion mass and the ratio of the ion charge to the proton charge), its density contribution will be underestimated by the same factor, and higher moments will also be affected. Effects of not discriminating among different ion species could be significant under some circumstances [B. Anderson and S. Fuselier, private comm., 1994]. However, as we discuss later, the effects on our results are not significant. Uncertainties due to particle-counting statistics affect the moment calculations but are reduced by averaging. Instrumental errors due to finite angular and energy resolutions and finite energy range are assessed by checking the sensitivity of the results to variations of the resolution and energy range. A vector flux-gate magnetometer on the satellite was sampled at 32 Hz. For our analysis, the magnetic field measurements were averaged over a spin period. In this study, we use 18 magnetosheath traversals by the satellite, each of which lasted about two hours. Each crossing occurred during the local time period of 8-14h while

the satellite was within 12° of the ecliptic plane.

We diagonalize the tensor

$$\langle \mathbf{T} \rangle_\tau \equiv \frac{m_p \int d^3 \mathbf{v} (\mathbf{v} - \langle \mathbf{u} \rangle_\tau)(\mathbf{v} - \langle \mathbf{u} \rangle_\tau)\langle f \rangle_\tau}{\langle n \rangle_\tau}, \quad (1)$$

where m_p=proton mass. Of the three eigenvalues, we identify one distinct eigenvalue (T_1) whose magnitude is most separated from that of the remaining two (T_2 and T_3). That is, $|T_1 - T_3| \geq |T_1 - T_2| \geq |T_2 - T_3|$. We define a unit vector $\hat{\eta}_1$ which is parallel to the principal axis associated with T_1; the ambiguity in the direction of $\hat{\eta}_1$ is removed by requiring $\hat{\eta}_1 \cdot \mathbf{B} \geq 0$. We denote the angle between $\hat{\eta}_1$ and $\mathbf{B}$ by θ_1; this angle, $\theta_1 \equiv \mathrm{acos}(\hat{\eta}_1 \cdot \mathbf{B}/B)$, only assumes values between 0 and $\pi/2$.

Results and Discussion

Figure 1 shows measured quantities averaged over 15-spin periods for the outbound traversal of the magnetosheath on Sept. 19, 1984, beginning after a magnetopause crossing (UT 16:11) and ending before a bow shock crossing (UT 18:28). The panels of the figure display: a) magnetic field strength, B; b) ion number density, n; c) number density of ions in the energy range 8-40 keV, n_2; d) ion bulk flow speed, u; e) eigenvalues T_1 (dashed line), T_2, and T_3 in units of 6×10^6 °K; f) angle between $\hat{\eta}_1$ and $\mathbf{B}$, θ_1; g) plasma beta, $\beta = 8\pi n T/B^2$, where $T = (T_1 + T_2 + T_3)/3$; h) $\delta B/B$, where δB is the rms fluctuation of B about its average over one satellite spin period; i) $T_\parallel$, $T_{\perp 1}$, and $T_{\perp 2}$ in units of 6×10^6 °K. $T_\parallel$, $T_{\perp 1}$ and $T_{\perp 2}$ are the diagonal elements of $\mathbf{T}$ in a coordinate system one axis of which is along $\mathbf{B}$. The orientation of the two axes perpendicular to $\mathbf{B}$ is chosen to diagonalize the 2x2 submatrix of $\mathbf{T}$ associated with those axes; $T_{\perp 1}$ and $T_{\perp 2}$ are the eigenvalues of that 2x2 submatrix. The full tensor $\mathbf{T}$ is not diagonal with respect to this coordinate system.

In Fig. 1e we see that T_2 and T_3 are usually nearly equal and quite distinct from T_1. This means that $\hat{\eta}_1$, which lies along the principal axis associated with T_1, is nearly a symmetry axis. We emphasize that the process of identifying a symmetry axis has not involved any reference direction at all, such as the direction of $\mathbf{B}$. In equilibrium and to lowest order in the gyroradius and the reciprocal cyclotron frequency, the ion pressure tensor is expected to be symmetric about the magnetic field direction when the plasma is anisotropic. Fig. 1f shows that θ_1, the instantaneous angle between the symmetry axis and the magnetic field, is not zero but lies near 15°, except during the period between UT 17:02 and UT 17:20 when there is a significant decrease in the magnetic field strength, with corresponding increases in n_2, β, and $\delta B/B$. These properties may correspond to typical conditions downstream of a quasi-parallel shock [e.g., Crooker et al., 1981]. During this period, as shown in Fig. 1i, $T_\parallel$ is not well separated from $T_{\perp 1}$ and $T_{\perp 2}$; however, T_1 is still distinct from T_2 and T_3.

In Figs. 2-4 we examine the distribution of values of the angle θ_1 and of the temperature anisotropy $A \equiv (T_2 + T_3)/2T_1$ for the entire set of 18 magnetosheath traversals. Fig. 2a is a scatter plot of θ_1 vs. A; and Fig. 2b is a histogram of the [number of occurrences/ $\sin(\theta_1)$] versus θ_1 with a bin width of 1°. The normalization by $\sin(\theta_1)$ accounts for the variation of solid angle with the polar angle (θ_1) and provides a true measure of the probability of the occurrence of θ_1. Each dot represents an average over 5 satellite spin periods. Cases when the temperature is less than 3×10^6 °K (25%) have been omitted in Fig. 2 in order to eliminate data affected by the limited angular resolution, and data for which n_2 is greater than $0.12\mathrm{cm}^{-3}$ (4%) have been omitted
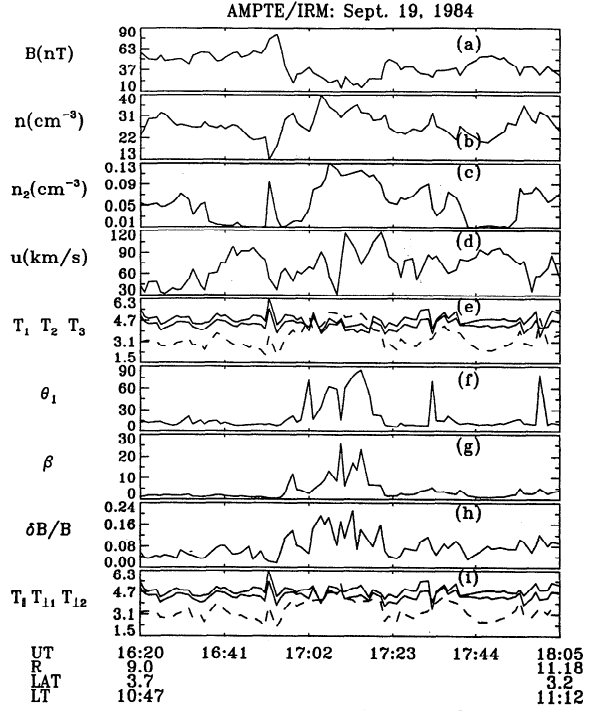

Figure 1. Outbound traversal of magnetosheath. From top to bottom, (a) the magnetic field strength, B; (b)the ion number density, n; (c)the partial density n_2 of energetic ions in the energy range 8 keV to 40 keV; (d) the ion bulk speed, u; (e) the three eigenvalues of $\mathbf{T}$: T_1 is plotted with dashed line; (f) θ_1, the angle between $\hat{\eta}_1$ and $\mathbf{B}$; (g) β, defined as $8\pi n T/B^2$; (h) $\delta B/B$ fractional rms fluctuation of B over one spin period; (i) the usual $T_\parallel$ (dashed line), $T_{\perp 1}$, and $T_{\perp 2}$.

in order to eliminate cases where ion energy range was not adequately covered by the particle detectors. These omissions do not affect the following features of Fig. 2: 1) Fig. 2b shows that the most probable value of θ_1 is not zero, but about 5°, 2) Fig. 2a shows a correlation of θ_1 with A. Adiabatic theory predicts to lowest order in the adiabatic parameter ϵ, the ratio of the gyroradius to the characteristic distance over which fields change, that the pressure tensor should be diagonal in a frame in which $\mathbf{B}$ is along one of the axes, the diagonal components being $p_\parallel, p_\perp, p_\perp$. This is a consequence of the distribution function being gyrotropic to lowest order in ϵ. To next order in ϵ, the off-diagonal components no longer vanish; there are also order-ϵ corrections to the diagonal components. Macmahon [1965] has given expressions for these corrections. If the higher-order, not-quite-diagonal, tensor is diagonalized, the new principal axes will not be parallel and perpendicular to $\mathbf{B}$.
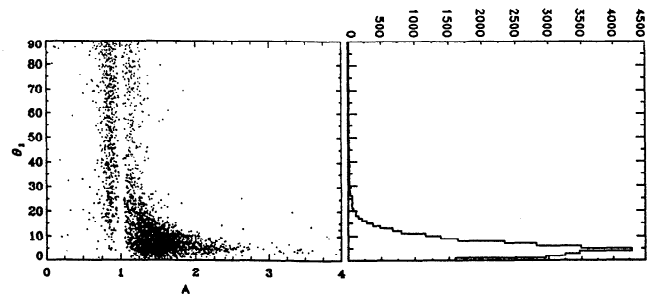

Figure 2. (a) Scatter plot of θ_1 vs. $A \equiv (T_2 + T_3)/2T_1$; (b) histogram of (number of occurrences)/ $\sin(\theta_1)$ vs. θ_1 with a bin width of 1°.
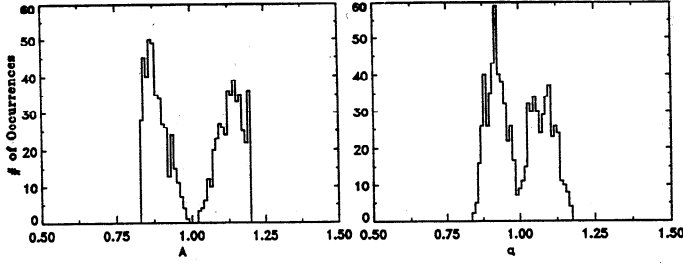
Figure 3. (a)Histogram of (number of occurrences) vs. A for $1/1.2 \leq A \leq 1.2$ with a bin width of 0.1; (b) histogram of (number of occurrences) vs. a for $1/1.2 \leq a \leq 1.2$ with a bin width of 0.1, where a is derived from triplets of random numbers.

In order to study the gap around $A = 1$ shown in Fig. 2a, which implies that the ion pressure tensor does not approach isotropy, we made a histogram of the number of occurrences versus A for $1/1.2 \leq A \leq 1.2$ (total of 679 dots), with a bin width of 0.1. This histogram, shown in Fig. 3a, shows no occurrences at $A = 1$. Even if the triples (T_1, T_2, T_3) in Fig. 3a were randomly distributed, there would be a minimum at $A = 1$ because the probability that three random numbers fall in the same bin is small. To assess the extent to which the gap at $A = 1$ in Fig. 3a could be produced by random numbers, we performed a computer experiment by generating 679 triplets (t_1, t_2, t_3) of random numbers on the interval $(1/1.2, 1.2)$. Ordering each triplet in the same way as were (T_1, T_2, T_3), an "anisotropy" $a \equiv (t_2 + t_3)/2t_1$ was calculated. A histogram of number of occurrences versus a for $1/1.2 \leq a \leq 1.2$ is shown in Fig. 3b. It is apparent that the gap in Fig. 3a cannot be accounted for by random statistics. Furthermore, repeating the experiment using data averaged over longer time windows ($\tau = 10, 20, 30, ...$), the gap in Fig. 3a does not change significantly, but the minimum in Fig. 3b becomes less and less pronounced as one would expect.

The observation of clusters of occurrences of $A < 1$ and $A > 1$ may have a physical explanation related to the condition of the bow shock. Most of the traversals in our data set occur near local noon. During a quasi-perpendicular shock (angle between **B** and the shock normal, $\theta_{BN}, \geq 45°$), the magnetic field in the sheath is compressed, and the particles' perpendicular energies increase as they penetrate the sheath in order to conserve the magnetic moment. In fact, Sckopke et al. [1990] found that in general $T_\perp/T_\parallel > 1$ for the "core" ion population downstream of quasi-perpendicular shocks. However, with a parallel shock ($\theta_{BN}=0$), the magnetic field upstream penetrates directly into the sheath without compression. Moreover, more energetic particles upstream enter the sheath [e.g., Crooker et al., 1981], increasing the β of the sheath
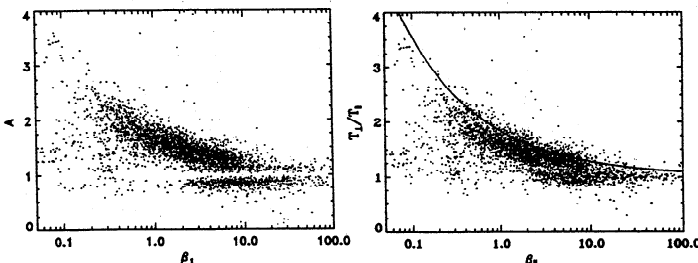
plasma. Under quasi-parallel conditions, the distribution may be skewed, and the anisotropy in the sheath might reflect that of the solar wind where $A < 1$ [Feldman et al., 1973]. We have examined each individual traversal and found that $A < 1$ usually corresponds to increases in energetic particles (n_2), β, and $\delta B/B$ and to a decrease in B, typical conditions downstream of a quasi-parallel shock. In any case, the plasma in the sheath is constantly supplied by the solar wind through the bow shock boundary, and the relaxation time of the collisionless plasma is sufficiently long that there is not enough time for relaxation to an isotropic state.

The same data used in Fig. 2 are displayed as a scatter plot of A versus $\beta_1 \equiv 8\pi n T_1/B^2$ in Fig. 4a. The gap at $A = 1$ and the correlation between A and β_1 are apparent. Fig. 4b shows a similar scatter plot of $T_\perp/T_\parallel$ versus $\beta_\parallel$, where $T_\perp = (T_{\perp 1} + T_{\perp 2})/2$. Anderson et al. [1994] studied similar scatter plots of AMPTE/CCE data in the magnetosheath adjacent to the magnetopause during highly compressed conditions. Although Fig. 4b is similar to Fig. 4a, it does not show the gap at $A = 1$.

We have done the same analysis with the electron pressure tensor, but in many cases the symmetry axis of the electron pressure tensor is parallel to the spin axis of the spacecraft. This instrumental effect invalidates such an analysis of the electron data. The ion pressure tensor does not suffer from this problem.

We now address the effects of not discriminating among different ion species. In general, the relationship between flux, $\Phi(E)$, and velocity distribution function, $f(v)$, is [Lyons and Williams, 1984]

$$\Phi(E) = (2E/m^2)f(v), \qquad (2)$$

where $E = \frac{1}{2}mv^2$. When there are both protons and He^{2+}, the total flux detected by the instrument, which is sensitive to E/q, is:

$$\Phi_{tot}(E) = (2E/m_p^2)f_p(v) + z_a(2E/m_a^2)f_a(v/\gamma), \quad (3)$$

where $\gamma = [(m_a/m_p)/z_a]^{1/2}$. The corresponding measured total velocity distribution function is

$$f(v) = f_p(v) + (z_a/(m_a/m_p)^2)f_a(v/\gamma). \qquad (4)$$

The moments n, **u** and **T** are computed from this velocity distribution. We modeled the magnetosheath plasma as 96% protons and 4% He^{2+}, with both species described by bi-Maxwellian distributions with drift velocities $\mathbf{u}_p$ and $\mathbf{u}_a$. The coordinate system has z-axis parallel to the background magnetic field and y-axis perpendicular to both drift velocities ($\mathbf{u}_p$ and $\mathbf{u}_a$ in the x-z plane). In the magnetosheath, the He^{2+} and proton thermal velocities are comparable, and $\mathbf{u}_p \approx \mathbf{u}_a$ [Fuselier et al., 1988]. Using this model to calculate the
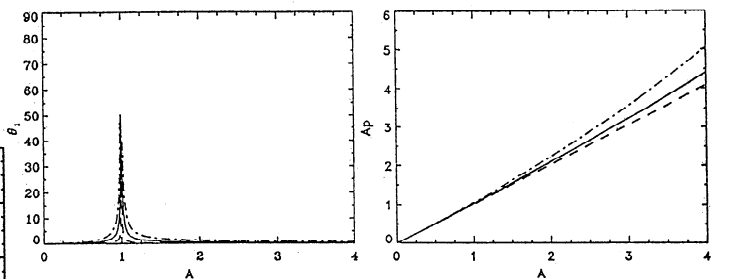

Figure 4. (a) Scatter plot of A vs. β_1; (b) scatter plot of $T_\perp/T_\parallel$ vs. $\beta_\parallel$, the curve is calculated from $T_\perp/T_\parallel = 1 + 0.85\beta_\parallel^{-0.48}$ [Anderson et al., 1994]

Figure 5. (a) Simulated results for θ_1 vs. A and (b) A_p vs. A. The parameters are described in the text: $T_{\perp p} = 300$ eV; $\lambda = u_p/(T_{\perp p}/m_p)^{1/2}$; $\theta_{BN} = 45°$; $\theta_{uB} = 45°$; $u_{\text{diff}} = u_p$. The proton temperature anisotropy $A_p = T_{\perp p}/T_{\parallel p}$ is varied from 0.02 to 6.0. The dashed, solid, and dotted-dashed lines correspond to λ=0.5, 1.0, 1.5, respectively.

moments for various parameters, we determined the parameters to which the results of Fig. 5 are most sensitive: (1) the ratio of proton drift speed to proton perpendicular thermal speed (λ); (2) the difference between the parallel drift speeds of the two species; and (3) the relative abundance of the two species.

To generate Fig. 5, we selected: $T_{\perp p} = 300$ eV; $\lambda = u_p/(T_{\perp p}/m_p)^{1/2} = 0.5, 1.0, 1.5$; angle between **B** and the shock normal, $\theta_{BN} = 45°$; the angle between **u** and **B**, $\theta_{uB} = 45°$; $u_{\perp a} - u_{\perp p} = 0$, $u_{\|a} - u_{\|p} = u_{\text{diff}} \cos(\theta_{BN})$, with $u_{\text{diff}} = u_p$. The proton temperature anisotropy $A_p = T_{\perp p}/T_{\|p}$ is varied from 0.02 to 6.0. In Fig. 5a, θ_1 is plotted vs. A; in Fig. 5b, A_p is plotted vs. A. The dashed, solid and dotted-dashed lines correspond to λ=0.5, 1.0, and 1.5, respectively. The two individually gyrotropic bi-Maxwellian distributions ($\theta_{1p} = \theta_{1a} = 0$) are not gyrotropic in combination ($\theta_1 \neq 0$) when they are interpreted as all protons by an instrument which is only sensitive to E/q. The same effect causes the proton temperature anisotropy A_p to be underestimated [first suggested by B. Anderson, private comm.] as shown Fig. 5b. However, the magnitudes of the effects illustrated in Figs. 5a and 5b are far too small to account for what we have observed (Fig. 1f and Fig. 2). The effects illustrated in Fig. 5 are larger for larger values of λ, but less than 15% (0.8%) of the data used in this paper have $\lambda > 1.0$ (1.2). The model also predicts a far smaller gap around $A = 1$ than observed (Fig. 3a).

Conclusions

Without theoretical assumptions, we have studied the ion pressure tensor in the magnetosheath. There is an instantaneous symmetry axis of the pressure tensor about an axis which is generally not parallel to the magnetic field, and this symmetry axis persists despite dynamical processes in the plasma which may be non-adiabatic. We have not made quantitative comparisons with the results of Macmahon [1965] because his expressions involve spatial gradients which we do not measure. The ion pressure tensor tends to stay away from isotropy; it is either oblate ($A > 1$, corresponding most likely to a quasi-perpendicular shock) or prolate ($A < 1$, corresponding most likely to a quasi-parallel shock). By checking the ruggedness of our results to angular resolution, energy resolution, and energy range, known instrument effects have been eliminated as causes of the observations. The fact that the particle detector does not distinguish ion species might be expected to produce similar results, but quantitative modeling shows that the magnitudes are far smaller than we observed, and analytic calculations support this conclusion [B. Anderson, private comm., 1994].

Because of the axisymmetry of the ion pressure tensor, a useful lowest-order form for modeling ion distribution functions might be $f(\mathbf{r}, v_1, v_2^2 + v_3^2, t)$, where v_1 is the velocity component along the symmetry axis, and v_2 and v_3 are two perpendicular components. This relation might provide a good basis for a more refined phenomenological description of the plasma. The corresponding reduction of the number of independent components of the heat flux tensor would simplify investigations of empirical closure relations involving third moments.

References

Anderson, B., S. Fuselier, S. Gary, and R. Denton, Magnetic spectral signatures in the Earth's magnetosheath and plasma depletion layer, *J. Geophys. Res.*, *99*, 5877, 1994.

Baumjohann, W. and G. Paschmann, Determination of the polytropic index in the plasma sheet, *Geophys. Res. Lett.*, *16*, 295, 1989.

Belmont, G. and C. Mazelle, Polytopic Indices in collisionless plasmas: theory and measurements, *J. Geophys. Res.*, *97*, 8327, 1992.

Chew, G., M. Goldberger, and F. Low, The Boltzmann equation and the one-fluid hydromagnetic equations in the absence of particle collisions, *Proc. Roy. Soc., Ser. A.*, *236*, 112, 1956.

Crooker, N., T. Eastman, L. Frank, E. Smith, and C. Russell, Energetic magnetosheath ions and the IMF orientation, *J. Geophys. Res.*, *86*, 4455, 1981.

Feldman, W. C., J. R. Asbridge, S. J. Bame, and H. R. Lewis, Empirical closure relation for the Vlasov moment equations, *Phys. Rev. Lett.*, *30*, 271, 1973.

Fuselier, S., E. Shelley, and D. Klumpar, AMPTE/CCE observations of shell-like He^{2+} and O^{6+} distributions in the magnetosheath, *Geophys. Res. Lett.*, *15*, 1333, 1988.

Hau, L.-N., T.-D. Phan, B. U. Ö. Sonnerup, and G. Paschmann, Double-polytropic closure in the magnetosheath, *Geophys. Res. Lett.*, *20*, 2255, 1993.

Hill, P., G. Paschmann, R. A. Treumann, W. Baumjohann, and N. Sckopke, Plasma and magnetic field behavior across the magnetosheath near local noon, *J. Geophys. Res.*, in press, 1994.

Huang, C. Y., C. K. Goertz, L. Frank, and G. Rostoker, Observational determination of the adiabatic index in the plasma sheet, *Geophys. Res. Lett.*, *16*, 563, 1989.

Lyons, L. R. and D. J. Williams, Quantitative aspects of magnetospheric physics, p.20-21, D. Reidel, Boston, 1984.

Mazelle, C. and G. Belmont, Determination of electron polytropic indices in the environment of comet P/Halley, *Geophys. Res. Lett.*, *20*, 157, 1993.

Macmahon, A., Finite gyro-radius corrections to the hydromagnetic equations for a Vlasov plasma, *The Phys. of Fluids*, *8*, 1840, 1965.

Phan, T.-D., G. Paschmann, W. Baumjohann, N. Sckopke, and H. Luchr, The magnetosheath region adjacent to the dayside magnetopause: AMPTE/IRM observations, *J. Geophys. Res.*, *99*, 121, 1994.

Sckopke, N., G. Paschmann, A. L. Brinca, C. Carlson, and H. Lühr, Ion thermalization in quasi-perpendicular shocks involving reflected ions, *J. Geophys. Res.*, *95*, 6337, 1990.

J. LaBelle, H. R. Lewis and X. Li, Dept. of Physics and Astronomy, Dartmouth College, Hanover, NH 03755-3258

T.-D. Phan, Herzberg Institute of Astrophysics, NRC, Ottawa, Ontario, Canada K1A 0R6

R. A. Treumann, Max-Planck-Institut für Extraterrestrische Physik, 8046 Garching, Germany